Original article

# Correlation between Standardized Uptake Value of $^{68}$Ga-DOTA-NOC Positron Emission Tomography/Computed Tomography and Pathological Classification of Neuroendocrine Tumors

**Chalermrat Kaewput, Subapriya Suppiah[1], SobhanVinjamuri[2]**

Department of Radiology, Division of Nuclear Medicine, Faculty of Medicine Siriraj Hospital, Mahidol University, Bangkok, Thailand, [1]Centre for Diagnostic Nuclear Imaging, Universiti Putra Malaysia, Selangor, Malaysia, [2]Department of Nuclear Medicine, Royal Liverpool University Hospital, Liverpool, UK

## Abstract

The aim of our study was to correlate tumor uptake of $^{68}$Ga-DOTA-NOC positron emission tomography/computed tomography (PET/CT) with the pathological grade of neuroendocrine tumors (NETs). $^{68}$Ga-DOTA-NOC PET/CT examinations in 41 patients with histopathologically proven NETs were included in the study. Maximum standardized uptake value ($SUV_{max}$) and averaged SUV $SUV_{mean}$ of "main tumor lesions" were calculated for quantitative analyses after background subtraction. Uptake on main tumor lesions was compared and correlated with the tumor histological grade based on Ki-67 index and pathological differentiation. Classification was performed into three grades according to Ki-67 levels; low grade: Ki-67 <2, intermediate grade: Ki-67 3–20, and high grade: Ki-67 >20. Pathological differentiation was graded into well- and poorly differentiated groups. The values were compared and evaluated for correlation and agreement between the two parameters was performed. Our study revealed negatively fair agreement between $SUV_{max}$ of tumor and Ki-67 index ($r$ = –0.241) and negatively poor agreement between $SUV_{mean}$ of tumor and Ki-67 index ($r$ = –0.094). $SUV_{max}$ of low-grade, intermediate-grade, and high-grade Ki-67 index is 26.18 ± 14.56, 30.71 ± 24.44, and 6.60 ± 4.59, respectively. Meanwhile, $SUV_{mean}$ of low-grade, intermediate-grade, and high-grade Ki-67 is 8.92 ± 7.15, 9.09 ± 5.18, and 3.00 ± 1.38, respectively. As expected, there was statistically significant decreased $SUV_{max}$ and $SUV_{mean}$ in high-grade tumors (poorly differentiated NETs) as compared with low- and intermediate-grade tumors (well-differentiated NETs). SUV of $^{68}$Ga-DOTA-NOC PET/CT is not correlated with histological grade of NETs. However, there was statistically significant decreased tumor uptake of $^{68}$Ga-DOTA-NOC in poorly differentiated NETs as compared with the well-differentiated group. As a result of this pilot study, we confirm that the lower tumor uptake of $^{68}$Ga-DOTA-NOC may be associated with aggressive behavior and may, therefore, result in poor prognosis.

**Keywords:** $^{68}$Ga-DOTA-NOC positron emission tomography/computed tomography, Ki-67, neuroendocrine tumors, standardized uptake value

## Introduction

Neuroendocrine tumors (NETs) are defined as epithelial neoplasms with predominant neuroendocrine differentiation and can arise in almost any organ of the body. They involve overexpression of receptors for regulatory peptides such as somatostatin and the presence of cellular structures for amine uptake and storage. Several prognostic factors have been studied. The prognostic value of several pathological (cytology, Ki-67

**Address for correspondence:**
Dr. Chalermrat Kaewput, Department of Radiology, Division of Nuclear Medicine, Faculty of Medicine Siriraj Hospital, 2 Prannok Road, Bangkoknoi, Bangkok 10700, Thailand.
E-mail: aung_med@hotmail.com

**Access this article online**

Quick Response Code:

Website: www.wjnm.org

DOI: 10.4103/wjnm.WJNM_16_17

This is an open access article distributed under the terms of the Creative Commons Attribution-NonCommercial-ShareAlike 3.0 License, which allows others to remix, tweak, and build upon the work non-commercially, as long as the author is credited and the new creations are licensed under the identical terms.

**For reprints contact:** reprints@medknow.com

**How to cite this article:** Kaewput C, Suppiah S, Vinjamuri S. Correlation between standardized uptake value of $^{68}$Ga-DOTA-NOC positron emission tomography/computed tomography and pathological classification of neuroendocrine tumors. World J Nucl Med 2018;17:34-40.

index) or biological (chromogranin A) factors is known in nonmetastatic disease but is less studied in metastatic disease.[1] NETs typically have a wide range of cellular differentiation. The presence of cell surface receptors appears to depend on tumor cell differentiation, with well-differentiated tumors exhibiting a greater affinity for somatostatin.[2]

Imaging plays a key role in the evaluation of these tumors including detection, staging, response assessment, and prognostication.[3] F-18 fludeoxyglucose positron emission tomography/computed tomography PET/CT has limited value in well-differentiated NETs as these tumors often have near normal glucose turnover.[4] $^{68}$Ga DOTA-conjugated peptide-binding somatostatin receptor (SSTR) has been widely used for localizing primary tumors and to detect sites of metastatic NETs (staging) as well as to select patients with metastatic disease for peptide receptor radionuclide therapy (PRRT).[5] PRRT can be successful in controlling symptoms because of excessive hormonal secretion and has also been shown to improve overall survival in patients with progressive or symptomatic NETs.[6] Their mechanism of uptake in neuroendocrine cells is due to the increased expression of SSTR and is also the basis of imaging with SSTR scintigraphy.[7]

In our study, we aimed to analyze the correlation between tumor uptake of $^{68}$Ga DOTANOC and Ki-67 index in patients with recurrent or metastatic NETs.

## Materials and Methods

### Study design and patients

We retrospectively reviewed the medical information of 41 patients (24 men and 17 women, age range: 22–84, mean age 61.1 years) who had histologically diagnosed NETs and underwent $^{68}$Ga-DOTA-NOC PET/CT examinations in the Department of Nuclear Medicine at the Royal Liverpool University Hospital between May 2013 and April 2016. Pathological diagnoses were confirmed by total resection ($n$ = 8) and tissue biopsy ($n$ = 33).

Images and the nonimaging data were anonymized at the time of re-analysis for tumor uptake by a member of the clinical care team. Since the current analysis is based on anonymized data and because the implications of the study do not have any direct implications to individual patients, additional informed consent for patients to participate in this study was not deemed necessary. All patients have been informed and have consented that their anonymized data could be used in research settings without the need for further consent.

### $^{8}$Ga-DOTA-NOC positron emission tomography/computed tomography imaging

$^{68}$Ga-DOTA-NOC PET/CT examinations were performed at 1 h after injection 200 MBq of $^{68}$Ga-DOTA-NOC which was conducted on a discovery ST16 PET/CT scanner (GE Healthcare, Milwaukee, USA). The whole body scan was performed from vertex to mid thighs (time of flight, 3 min list mode per bed position). Low-dose CT acquisition was performed with 120 kV, 80 mA, 0.8 s per CT rotation. CT data were used for attenuation correction. Studies were interpreted on a Hermes Multimodality workstation using Hybrid Viewer software (Hermes Medical Solutions, Stockholm, Sweden).

### Imaging interpretation

The $^{68}$Ga-DOTA-NOC PET/CT images were interpreted retrospectively by an experienced nuclear medicine physician. PET images were evaluated both qualitatively and semiquantitatively. At first, the maximum intensity projection images were visually examined in varying scales, and then each single transverse slice was looked over from vertex to the mid thighs in combination with the corresponding CT image and the fused image slice. Each lesion showing a focal abnormal tracer uptake was recorded by a slice number and anatomical localization, and any lesion with intensity greater than background which could not be explained by physiological activity was considered to be indicative of tumor tissue. For semiquantitative analysis of the lesions, volume of interests (VOIs) was drawn around the largest and/or the lesion with the highest pathological tracer accumulation. This was clarified as "main tumor lesion" in each patient. Maximum standardized uptake value ($SUV_{max}$) and average SUV $SUV_{mean}$ were calculated and tabulated.

### Quantification analysis of tumor uptake on $^{68}$Ga-DOTA-NOC positron emission tomography/computed tomography

For quantification of relative tumor uptake, VOIs were drawn on all transverse consecutive PET slices along the contour of the "main tumor lesion." The outline was based on visual assessment as per CT images. The $SUV_{max}$ and $SUV_{mean}$ were generated by automatic software (Hermes Multimodality).

To provide some normalization and to correct for background activity, we chose a nonaffected vertebral body as a normal reference. $SUV_{max}$ of tumor was derived after normalization with $SUV_{max}$ of the "normal" vertebral reference, whereas $SUV_{mean}$ of tumor was derived after normalization with $SUV_{mean}$ of the "normal" vertebral reference. VOIs of main tumor lesion and vertebral reference were re-processed using Hermes Hybrid Viewer software and are shown in Figure 1.

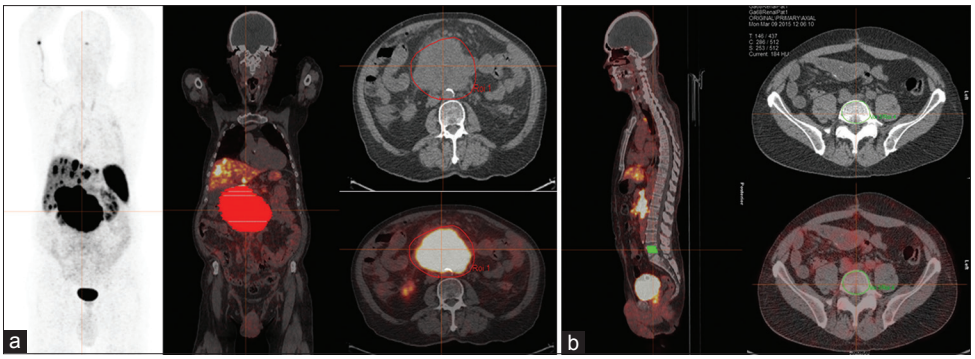


**Figure 1:** Volume of interest was drawn manually on all transverse consecutive positron emission tomography slices along the contour of "Main tumor lesion" (a) and normal vertebral references (b)

Quantitative assessment of tumor uptake on $^{68}$Ga-DOTA-NOC PET/CT was performed by an experienced nuclear medicine physician with each procedure repeated twice to reduce errors.

$SUV_{max}$ (mean) of main tumor lesions = $SUV_{max}$ (mean) of tumor – $SUV_{max}$ (mean) of normal vertebral reference

## Histopathological analysis

All NETs were graded as part of the routine workup with routine interventions including surgical resection, endoscopic biopsies, or ultrasound-guided biopsies. Pathologists were unaware of PET findings. We obtained the histological findings including the histological type and Ki-67 index of the primary tumor or metastatic sites. All NETs were classified into high, intermediate, and low-grade tumors according to the tumor histology report which were based on recent consensus statements of the European NET Society[8,9] and WHO classification,[10] using Ki-67 index or mitotic rate. Ki-67 index was expressed as the percentage of positive cells which were classified as low grade, <3%; intermediate grade, 3%–20%; and high grade, >20%. On the basis of this system, low and intermediate grades were classified as well-differentiated tumors, whereas high-grade tumors were classified as poorly differentiated tumors.

## Statistical analysis

Categorical data were expressed as numbers and percentages, whereas continuous variables were expressed as the mean and range. The Spearman correlation coefficient ($r$) was used to evaluate correlation and the agreement between $SUV_{max}$ of main tumor lesion in $^{68}$Ga-DOTA-NOC PET/CT and Ki-67 index and between $SUV_{mean}$ of the main tumor lesion in $^{68}$Ga-DOTA-NOC PET/CT and Ki-67 index. Scatter plots were also used to determine the correlation between the two datasets. The statistical differences of SUVs among each group of tumor grade were determined using Kruskal–Wallis test to determine the specific differences between the three groups when $P < 0.05$. Box and whisker plots of $SUV_{max}$ and $SUV_{mean}$ of main tumor lesions and each group of Ki-67 index were constructed. All analyses were conducted using the SPSS software version 22 (IBM Corporation, Armonk, NY, USA).

# Results

## Patient characteristics

The study included 41 patients (24 males and 17 females). Primary tumor sites included pancreas (29.3%), small bowel (24.4%), and stomach (2.4%). The primary site could not be identified in 43.9%. All patients had metastatic disease, with the most common location being the liver (58.5%), followed by regional lymph nodes (51.2%) and bone (31.7%). Histologic evaluation revealed well-differentiated ($n$ = 38) and poorly differentiated NETs ($n$ = 3). Patient characteristics are described in more detail in Tables 1 and 2.

## Correlation between standardized uptake value of main tumor lesions and Ki-67

$SUV_{max}$ of low-, intermediate-, and high-grade tumors is 26.18 ± 14.56, 30.71 ± 24.44, and 6.60 ± 4.59, respectively. Meanwhile, $SUV_{mean}$ of low-, intermediate-, and high-grade tumors is 8.92 ± 7.15, 9.09 ± 5.18, and 3.00 ± 1.38, respectively as described in Table 3. Correlation of $SUV_{max}$ and $SUV_{mean}$ and Ki-67 is shown in Figures 2 and 3, respectively. Correlation between $SUV_{max}$ and $SUV_{mean}$ of main tumor lesion and Ki-67 is −0.241 and −0.094, respectively. Box and whisker plots of $SUV_{max}$ and $SUV_{mean}$ of main tumor lesions and each group of Ki-67 were constructed [Figures 4 and 5]. On comparison of tumor SUV of $^{68}$Ga-DOTA-NOC and Ki-67 index, there was statistically significant decreased $SUV_{max}$ in high-grade tumor (poorly differentiated NETs) as compared with low- ($P$ = 0.014) and intermediate-grade ($P$ = 0.010) tumor (well-differentiated NETs) but no significant difference of $SUV_{max}$ between low and intermediate grades ($P$ = 0.850). For $SUV_{mean}$, there was also statistically significant decreased $SUV_{mean}$ in high-

**Table 1: Patients characteristic, tumor localizations, Ki-67 index, tumor grade and tracer uptake**

| Patient number | Primary tumor | Sites of main tumor lesion | Method of tissue collection | Ki-67-index | WHO grade | $SUV_{max}$ of main tumor lesion | $SUV_{mean}$ of main tumor lesion |
|---|---|---|---|---|---|---|---|
| 1 | Small bowel | Liver | Bowel resection | 2 | 1 | 22.9 | 10 |
| 2 | Pancreas | Pancreas | Whipple operation | 1 | 1 | 15.3 | 4 |
| 3 | Unknown | Liver | Liver biopsy | 12 | 2 | 19.8 | 9.8 |
| 4 | Small bowel | Small bowel | Bowel resection | 0.5 | 1 | 27.9 | 5.7 |
| 5 | Unknown | Liver | Liver biopsy | 0.5 | 1 | 30.1 | 7.1 |
| 6 | Small bowel | Small bowel | Small bowel biopsy | 4 | 2 | 34.6 | 13 |
| 7 | Small bowel | Small bowel | Small bowel biopsy | 4 | 2 | 24.8 | 10.4 |
| 8 | Unknown | Liver | Liver biopsy | 5 | 2 | 28.8 | 9.7 |
| 9 | Unknown | Liver | Liver biopsy | 10 | 2 | 11.5 | 4.7 |
| 10 | Pancreas | Pancreas | Whipple operation | 1.8 | 1 | 68.3 | 18.3 |
| 11 | Pancreas | Pancreas | EUS with biopsy | 18 | 2 | 45.2 | 8.7 |
| 12 | Pancreas | Pancreas | ERCP with FNA | 40 | 3 | 11.9 | 4.6 |
| 13 | Pancreas | Pancreas | Whipple operation | 3 | 2 | 31.2 | 4.8 |
| 14 | Pancreas | Pancreas | EUS with biopsy | 1 | 1 | 41.2 | 12.5 |
| 15 | Pancreas | Pancreas | EUS with biopsy | 2 | 1 | 47.8 | 33.8 |
| 16 | Unknown | Liver | Liver biopsy | 32 | 3 | 4.1 | 2.3 |
| 17 | Pancreas | Pancreas | Pancreatic resection | 18 | 2 | 8.7 | 3.9 |
| 18 | Unknown | Liver | Liver biopsy | 18 | 2 | 22 | 9.3 |
| 19 | Unknown | Mesenteric node | Node biopsy | 0.5 | 1 | 29.1 | 10.2 |
| 20 | Pancreas | Pancreas | EUS with biopsy | 5 | 2 | 103.8 | 25.2 |
| 21 | Small bowel | Liver | Bowel resection | 5.1 | 2 | 17.4 | 7.9 |
| 22 | Stomach | Stomach | FNA stomach | 9 | 2 | 82.2 | 17.4 |
| 23 | Unknown | Liver | Liver biopsy | 2.5 | 1 | 30.8 | 11.9 |
| 24 | Unknown | Liver | Liver biopsy | 2 | 1 | 23.2 | 6.4 |
| 25 | Unknown | Liver | Liver biopsy | 2 | 1 | 18.5 | 9.8 |
| 26 | Unknown | Liver | Liver biopsy | 10 | 2 | 22.1 | 8.1 |
| 27 | Unknown | Liver | Liver biopsy | 20 | 2 | 13.5 | 6.1 |
| 28 | Small bowel | Small bowel | Small bowel biopsy | 3 | 2 | 28 | 10.8 |
| 29 | Unknown | Liver | Liver biopsy | 2 | 1 | 23 | 7.6 |
| 30 | Small bowel | Small bowel | Small bowel biopsy | 5 | 2 | 37.3 | 8.8 |
| 31 | Small bowel | Small bowel | Small bowel biopsy | 1 | 1 | 17.3 | 5 |
| 32 | Pancreas | Pancreas | EUS with biopsy | 1 | 1 | 34.6 | 6.7 |
| 33 | Unknown | Liver | Liver biopsy | 10 | 2 | 32.2 | 5.3 |
| 34 | unknown | lung | Lung biopsy | 1 | 1 | 17.4 | 3.4 |
| 35 | Pancreas | Pancreas | EUS with biopsy | 1 | 1 | 20.5 | 3.7 |
| 36 | Unknown | Lung | Lung biopsy | 20 | 2 | 8.1 | 3.9 |
| 37 | Small bowel | Small bowel | EUS with biopsy | 1 | 1 | 5.9 | 3.3 |
| 38 | Unknown | Lung | Lung biopsy | 75 | 3 | 3.8 | 2.1 |
| 39 | Small bowel | Small bowel | Small bowel biopsy | 1 | 1 | 14.4 | 6.6 |
| 40 | Pancreas | Pancreas | Pancreatic resection | 1 | 1 | 9.3 | 3.5 |
| 41 | Unknown | Liver | Liver biopsy | 5 | 2 | 12.3 | 5 |

$SUV_{max}$: Maximum standardized uptake value; $SUV_{mean}$: Averaged standardized uptake value; EUS: Endoscopic ultrasound; FNA: Fine-needle aspiration; ERCP: Endoscopic retrograde cholangiopancreatography

grade tumor (poorly differentiated NETs) as compared with low- ($P = 0.025$) and intermediate-grade ($P = 0.010$) tumor (well-differentiated NETs) but no significant difference of $SUV_{mean}$ between low and intermediate grades ($P = 0.516$).

## Discussion

The grade of a tumor refers to its biological aggressiveness which has been accepted as a powerful indicator for prognosis in various tumors. NETs are defined as epithelial neoplasms with predominant neuroendocrine differentiation and can arise in almost any organ of the body. The grading system of NETs is based on the rate of proliferation which is defined by the number of mitoses per ten high-power microscopic fields or 2 $mm^2$ (mitotic rate) or as the percentage of tumor cells immunolabeled for positively for the Ki-67 antigen (Ki-67 index).[11] NETs can also be classified based on differentiation, which refers to the extent to which cancerous or neoplastic cells resemble normal cells. Patients with high-grade tumors have turnover with high aggressive nature and can progress rapidly, whereas others can remain stable for a long time. It is important to distinguish between rapidly

**Table 2: Baseline patients characteristic (*n*=41)**

| Characteristic | *n* (%) |
|---|---|
| Sex | |
| Male | 24 (58.5) |
| Female | 17 (41.4) |
| Age at diagnosis (years), mean±SD (maximum-minimum) | 61.12±13.62 (84-22) |
| Body weight (kg), mean±SD (maximum-minimum) | 76.26±18.75 (117-53) |
| Tumor grade (Ki-67) | |
| Low grade (<3) | 19 (46.3) |
| Intermediate grade (3-20) | 19 (46.3) |
| High grade (>20) | 3 (7.4) |
| Site of primary site | |
| Pancreas | 12 (29.3) |
| Small bowel | 10 (24.4) |
| Stomach | 1 (2.4) |
| Unknown | 18 (43.9) |
| Site of metastasis | |
| Liver | 24 (58.5) |
| Lymph nodes | 21 (51.2) |
| Bone | 13 (31.7) |
| Peritoneum | 6 (14.6) |
| Lung | 3 (7.3) |
| Adrenal gland | 1 (2.4) |
| Source of histopathology | |
| Pancreatic resection/Whipple's operation | 5 (12.2) |
| Small bowel resection | 3 (7.3) |
| Tissue biopsy | |
| Liver | 14 (34.2) |
| Pancreas | 7 (17.1) |
| Small bowel | 7 (17.1) |
| Lung | 3 (7.3) |
| Stomach | 1 (2.4) |
| Intra-abdominal mass | 1 (2.4) |
| Organ of main tumor lesions | |
| Liver | 16 (39.0) |
| Pancreas | 12 (29.3) |
| Small bowel | 8 (19.5) |
| Lung | 3 (7.3) |
| Stomach | 1 (2.4) |
| Mesenteric nodes | 1 (2.4) |
| Scan parameter | |
| Dose of $^{68}$Ga-DOTA-NOC (MBq) mean±SD (maximum-minimum) | 124.62±22.42 |
| Time/bed (s), mean±SD (maximum-minimum) | 193.90±27.73 |
| Uptake time (min), mean±SD (maximum-minimum) | 64.66±8.67 |

SD: Standard deviation

progressive tumors and relatively stable tumors because treatment for aggressive tumors can have significant long-term toxicity and moderate efficacy.[12]

$^{68}$Ga-DOTA-NOC PET/CT has been shown to have high diagnostic accuracy for the detection of primary and metastatic disease in patients with GEP-NETs.[13,14] In our study, we found no significant correlation between

**Table 3: Maximum standardized uptake value and averaged standardized uptake value of main tumor lesions in each grade of tumors**

| Tumor grade | Mean±SD | |
|---|---|---|
| | $SUV_{max}$ of main tumor lesions | $SUV_{mean}$ of main tumor lesions |
| Low (*n*=19) | 26.18±14.56 | 8.92±7.15 |
| Intermediate (*n*=19) | 30.71±24.44 | 9.09±5.18 |
| High (*n*=3) | 6.60±4.59 | 3.00±1.38 |

$SUV_{max}$: Maximum standardized uptake value; $SUV_{mean}$: Averaged standardized uptake value; SD: Standard deviation

tumor $SUV_{max}$ of $^{68}$Ga-DOTA-NOC and Ki-67 index ($r$ = −0.241) and between tumor $SUV_{mean}$ of $^{68}$Ga-DOTA-NOC and Ki-67 index ($r$ = −0.094). However, our results show significantly higher tumor $SUV_{max}$ of $^{68}$Ga-DOTA-NOC in low-grade ($SUV_{max}$ of 26.18) with lower tumor $SUV_{max}$ in high-grade tumors ($SUV_{max}$ of 6.60). In the previous study of Kayani *et al*.,[15] they also showed comparable results, and that there is greater uptake of $^{68}$Ga DOTATATE in low-grade NETs (median $SUV_{max}$ of 29), whereas high-grade tumors had lower uptake (median $SUV_{max}$ of 4.3). When we compared tumor $SUV_{mean}$ in our study, there is a lower uptake in high-grade tumors ($SUV_{mean}$ of 8.92) as compared with low-grade tumors ($SUV_{mean}$ of 3.00), but the difference was not so much as with tumor $SUV_{max}$. As expected, $SUV_{max}$ is a more accurate estimation of the true SUV than $SUV_{mean}$. In addition, $SUV_{max}$ has a significantly improved reproducibility as compared to $SUV_{mean}$. A concern with the use of $SUV_{max}$ is that it is based on a reported value for a lesion with perhaps only one pixel. Whereas $SUV_{mean}$ is used in certainty boundary definition of region of interests with no evidence of resolution loss.[16] We sought to reduce the errors associated with variable injected activities, variable imaging times after injection and possible variation in body mass by "subtracting" or "normalizing" with a noninvolved body part that was reproducible between studies. We decided to choose a discrete noninvolved vertebral body confirmed on PET as well as the CT components of the PET/CT study. We sought to further reduce errors by repeating the measurements twice and ensuring conformity of results.

On comparison of SUV of $^{68}$Ga-DOTA-NOC and Ki-67 index, there was statistically significant decreased $SUV_{max}$ and $SUV_{mean}$ in high-grade tumors (poorly differentiated NETs) as compared with low- and intermediate-grade tumor (well-differentiated NETs). In patients with high-grade metastatic with low tracer uptake, there is often limited SSTR expression. Tumor grade influenced tracer uptake, and SUV values of $^{68}$Ga-labelled peptide SSTR correlate inversely with the grade of tumor.[17] The presence of cell surface receptors appears to depend on tumor cell differentiation, with well-differentiated (low grade) tumors exhibiting a

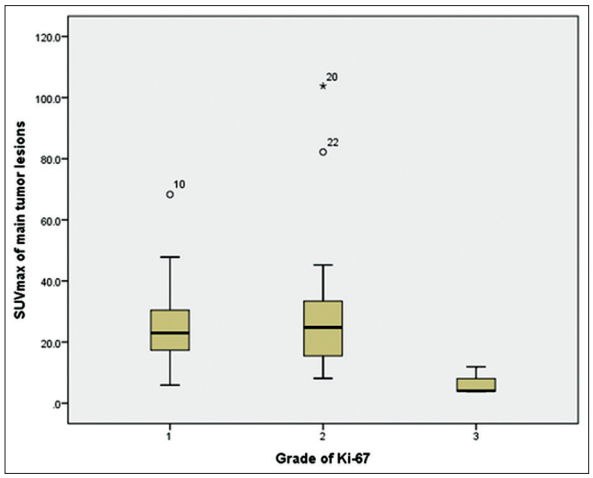


**Figure 2:** Box and whisker plot of different maximum standardized uptake value and grades of tumor

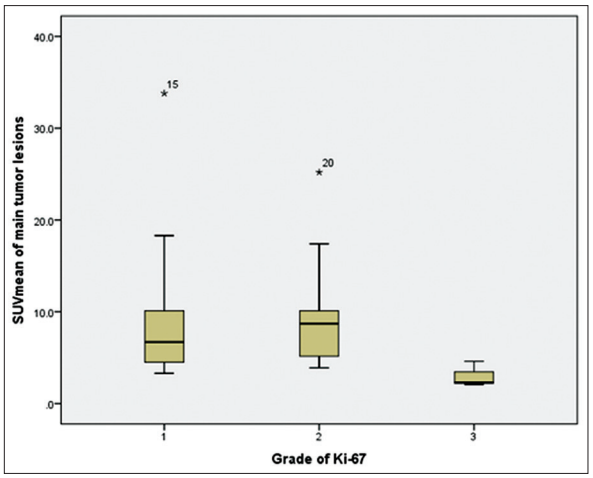


**Figure 3:** Box and whisker plot of different averaged standardized uptake value and grades of tumor

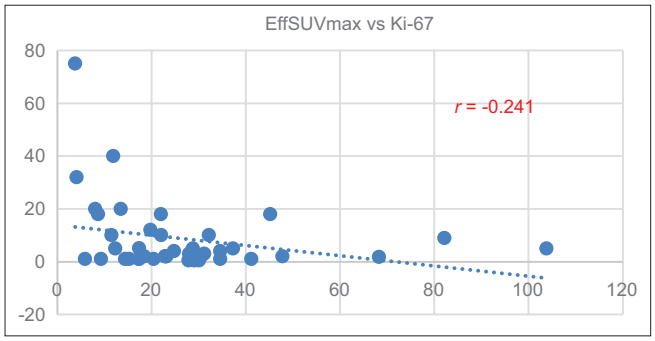


**Figure 4:** Correlation of maximum standardized uptake value and Ki-67 index

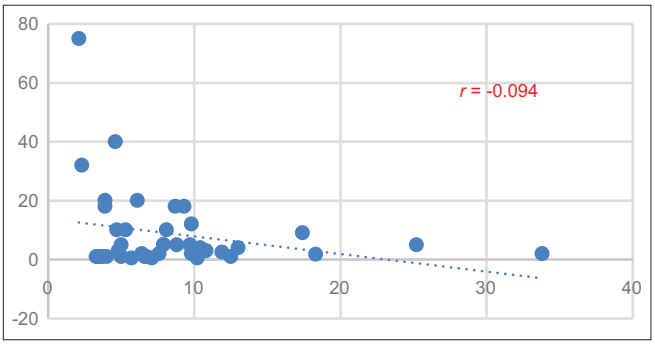


**Figure 5:** Correlation of averaged standardized uptake value and Ki-67 index

greater affinity for somatostatin. As a result of this pilot study, we suggest that the lower tumor uptake may be associated with aggressive tumor behavior that has prognosis relevance. However, it is difficult to establish a correlation between tracer avidity and histopathological grade of tumors because in many patients in our study, there were a large number of tumors lesions, often multiple lesions in the same organ (such as liver metastases) and variable tracer uptake was even seen within the same lesion site. These findings suggest the wide spectrum of differentiation of NETs, heterogeneity of cellular differentiation within the same tumor mass, and also reflect the potential ability of PET to map these cellular characteristics.

Although tumor grade and proliferation appeared to be related to tumor $^{68}$Ga-DOTA-NOC uptake, there were two patients (No.37 and 40) with low-grade NETs that showed low tumor uptake. The low tumor uptake ($SUV_{max}$ of 5.9) in one patient with recurrent NETs at duodenum with Ki-67 index of one from endoscopic fine-needle aspiration (FNA) of duodenum was observed [Figure 6]. It is possible that the FNA site may not fully reflect the true pathological grade of a patient with heterogeneity of cellular differentiation within the same tumor mass and this may also reflect the potential ability of $^{68}$Ga-labeled SSTR PET/CT to map these cellular characteristics. Another one patient with diagnosed recurrent NETs at the head of pancreas based on progressive imaging feature as seen on the follow-up CT scan with Ki-67 index of 1%. It also showed low tumor uptake ($SUV_{max}$ of 9.3) which is possible due to small tumor volume with the main proportion of necrotic tissue which may have then resulted in a lack of detectable tracer avidity.

There are some limitations to our study. First, our study population is small. The sample size in each group was not equal with the smallest number in high grade and may be insufficient to make conclusive statements on the correlation between $^{68}$Ga-DOTA-NOC uptake and pathological correlation. Second, in many patients, there were a large number of tumor lesions, often with multiple lesions in the same organ. Moreover, heterogeneous uptake within tumor lesions indicates histological findings from only one site and may not fully reflect *in vivo* tumor heterogeneity. Another limitation is that there was no follow-up period to confirm prognosis and survival of these patients.

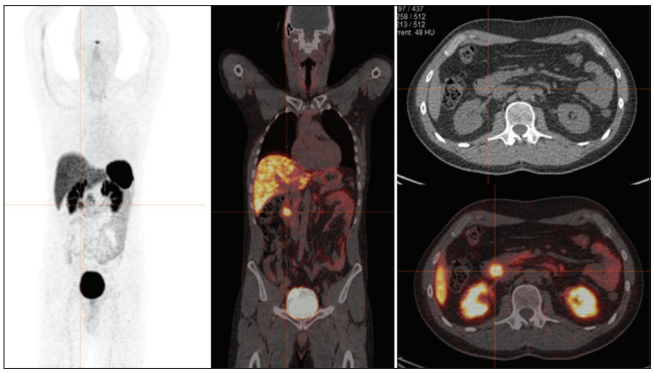

**Figure 6:** A 41-year-old male with recurrent neuroendocrine tumor at duodenum. $^{68}$Ga-DOTA-NOC positron emission tomography shows abnormal focal tracer uptake at duodenum (maximum standardized uptake value of 5.9) without other definite evidence of abnormal tracer uptake. Ki-67 index from endoscopic fine-needle aspiration of duodenum was 1%

## Conclusion

In our study, we found that tumor uptake of $^{68}$Ga-DOTA-NOC PET/CT is not correlated with the histological grade of NETs. However, there was statistically significant decreased tumor uptake of $^{68}$Ga-DOTA-NOC in poorly differentiated NETs which may be suggestive of aggressive tumor behavior and also reflects on the potential ability of PET/CT to map heterogeneous cellular characteristics rather than relying on histological information from only one sample.

### Financial support and sponsorship
Nil.

### Conflicts of interest
There are no conflicts of interest.

## References

1. Söreide JA, van Heerden JA, Thompson GB, Schleck C, Ilstrup -DM, Churchward M. Gastrointestinal carcinoid tumors: Long-term prognosis for surgically treated patients. World J Surg 2000;24:1431-6.
2. Ezziddin S, Logvinski T, Yong-Hing C, Ahmadzadehfar H, Fischer HP, Palmedo H, *et al.* Factors predicting tracer uptake in somatostatin receptor and MIBG scintigraphy of metastatic gastroenteropancreatic neuroendocrine tumors. J Nucl Med 2006;47:223-33.
3. Kuruva M, Bartel T, Osmany S. PET in Evaluation of Neuroendocrine Tumors. Available from: http://www.snmmi.files.cms plus.com/ACNM/010_PET%20in%20neuroendocrine%20tumors%20for%20Spotlights%20with%20Simin%20edits%207-27-15.pdf. [Last cited on 2016 Nov 16].
4. Belhocine T, Foidart J, Rigo P, Najjar F, Thiry A, Quatresooz P, *et al.* Fluorodeoxyglucose positron emission tomography and somatostatin receptor scintigraphy for diagnosing and staging carcinoid tumours: Correlations with the pathological indexes p53 and Ki-67. Nucl Med Commun 2002;23:727-34.
5. Mojtahedi A, Thamake S, Tworowska I, Ranganathan D, Delpassand ES. The value of (68)Ga-DOTATATE PET/CT in diagnosis and management of neuroendocrine tumors compared to current FDA approved imaging modalities: A review of literature. Am J Nucl Med Mol Imaging 2014;4:426-34.
6. Vinjamuri S, Gilbert TM, Banks M, McKane G, Maltby P, Poston G, *et al.* Peptide receptor radionuclide therapy with (90) Y-DOTATATE/(90)Y-DOTATOC in patients with progressive metastatic neuroendocrine tumours: Assessment of response, survival and toxicity. Br J Cancer 2013;108:1440-8.
7. Garin E, Le Jeune F, Devillers A, Cuggia M, de Lajarte-Thirouard AS, Bouriel C, *et al.* Predictive value of 18F-FDG PET and somatostatin receptor scintigraphy in patients with metastatic endocrine tumors. J Nucl Med 2009;50:858-64.
8. Rindi G, Klöppel G, Alhman H, Caplin M, Couvelard A, de Herder WW, *et al.* TNM staging of foregut (neuro) endocrine tumors: A consensus proposal including a grading system. Virchows Arch 2006;449:395-401.
9. Rindi G, Klöppel G, Couvelard A, Komminoth P, Körner M, Lopes JM, *et al.* TNM staging of midgut and hindgut (neuro) endocrine tumors: A consensus proposal including a grading system. Virchows Arch 2007;451:757-62.
10. Rindi G, Arnold B, Bosman FT. Nomenclature and classification of neuroendocrine neoplasms of the digestive system. In: Bosman FT, Hruban RH, Theise ND, editors. WHO Classification of Tumors of the Digestive System. Lyon, France: IARC; 2010. p. 13-4.
11. Klimstra DS, Modlin IR, Coppola D, Lloyd RV, Suster S. The pathologic classification of neuroendocrine tumors: A review of nomenclature, grading, and staging systems. Pancreas 2010;39:707-12.
12. Öberg K, Knigge U, Kwekkeboom D, Perren A; ESMO Guidelines Working Group. Neuroendocrine gastro-entero-pancreatic tumors: ESMO Clinical Practice Guidelines for diagnosis, treatment and follow-up. Ann Oncol 2012;23 Suppl 7:vii124-30.
13. Kwekkeboom DJ, Kam BL, van Essen M, Teunissen JJ, van Eijck CH, Valkema R, *et al.* Somatostatin-receptor-based imaging and therapy of gastroenteropancreatic neuroendocrine tumors. Endocr Relat Cancer 2010;17:R53-73.
14. Wild D, Bomanji JB, Benkert P, Maecke H, Ell PJ, Reubi JC, *et al.* Comparison of 68Ga-DOTANOC and 68Ga-DOTATATE PET/CT within patients with gastroenteropancreatic neuroendocrine tumors. J Nucl Med 2013;54:364-72.
15. Kayani I, Bomanji JB, Groves A, Conway G, Gacinovic S, Win T, *et al.* Functional imaging of neuroendocrine tumors with combined PET/CT using 68Ga-DOTATATE (DOTA-DPhe1,Tyr3-octreotate) and 18F-FDG. Cancer 2008;112:2447-55.
16. Kinahan PE, Fletcher JW. Positron emission tomography-computed tomography standardized uptake values in clinical practice and assessing response to therapy. Semin Ultrasound CT MR 2010;31:496-505.
17. Naswa N, Sharma P, Gupta SK, Karunanithi S, Reddy RM, Patnecha M, *et al.* Dual tracer functional imaging of gastroenteropancreatic neuroendocrine tumors using 68Ga-DOTA-NOC PET-CT and 18F-FDG PET-CT: Competitive or complimentary? Clin Nucl Med 2014;39:e27-34.